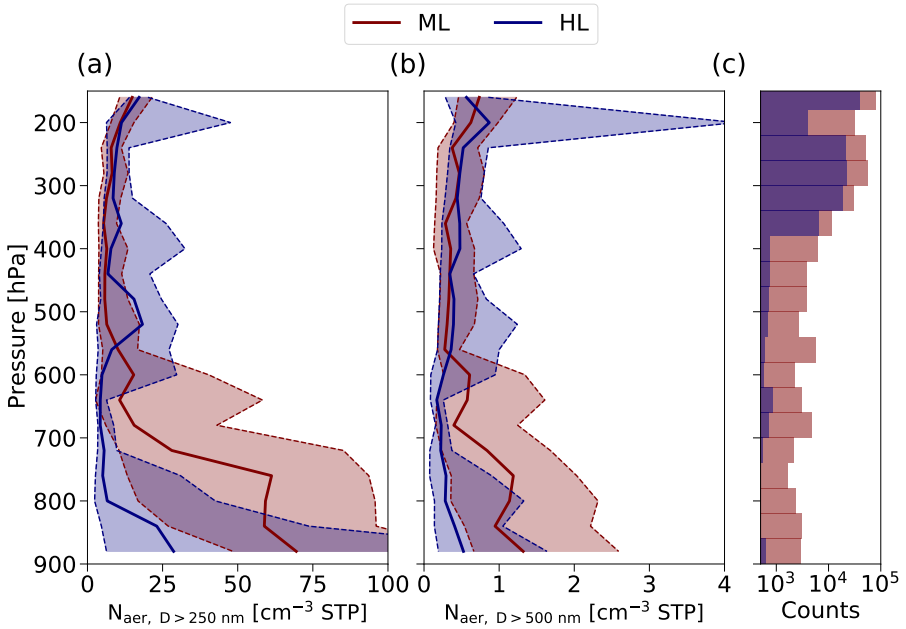

Figure S1. Same as Fig. 1 but comparing the particle size ranges (a) $D > 250$ nm and (b) $D > 500$ nm from the OPC measurements. Median profiles are indicated with solid lines, the areas between the 25^{th} and 75^{th} percentiles are filled and indicated within dashed lines. (c) Number of observations per pressure bin of 40 hPa each.

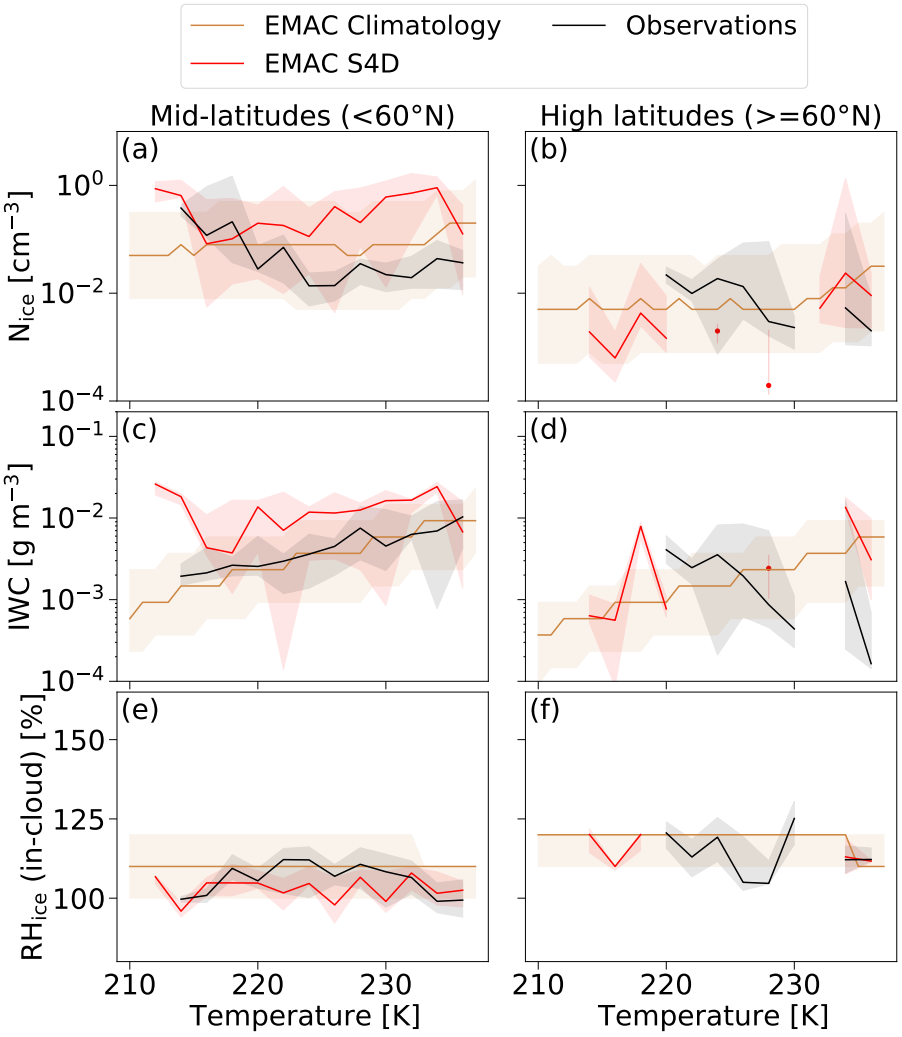

Figure S2. As in Fig. 5, but without the all-data panels and with a model climatological average (brown) for June-July 2014-2021 included as reference. Climatological model output was not obtained applying the diagnostic submodel S4D (Sampling in 4 Dimensions; Jöckel et al. 2010) along the flight tracks, but instead by averaging over the latitude, longitude and altitude range of the CIRRUS-HL flights.

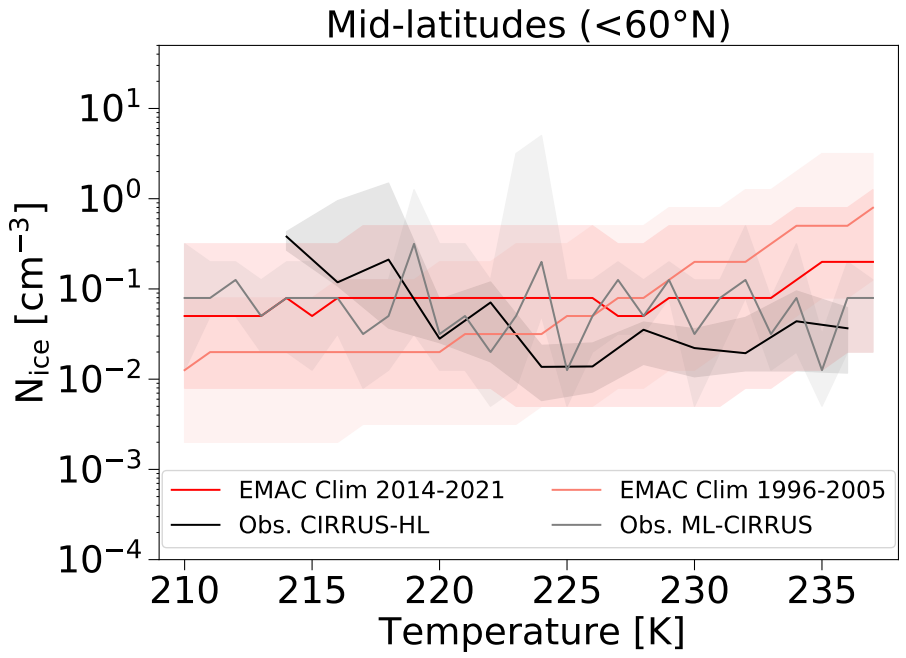

Figure S3. Similar as Fig. 5 (b) but comparing observations from CIRRUS-HL (black) and ML-CIRRUS (gray) with climatological model averages over the corresponding periods: 2014-2021 for CIRRUS-HL (red) and 1996-2005 for ML-CIRRUS (salmon). Observational and model data for ML-CIRRUS are taken from the study by Righi et al., (2020).

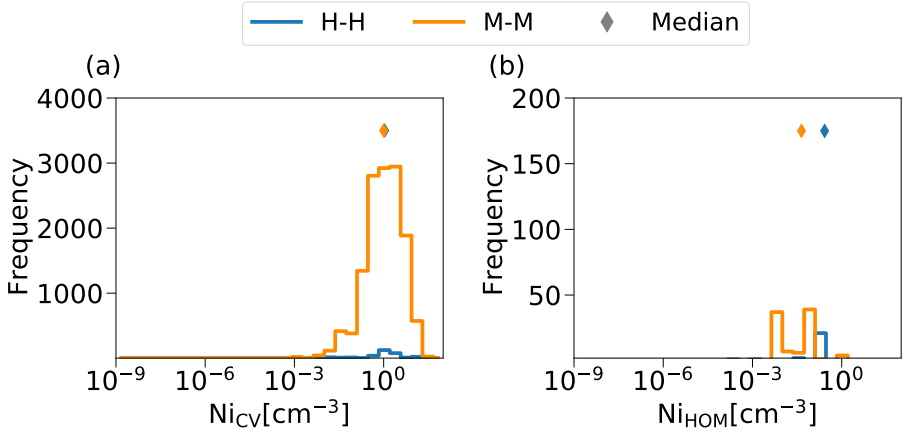

Figure S4. Absolute frequency distribution of newly formed ice crystals from (a) convection (CV), and (b) homogeneous freezing (HOM) along all backward trajectories of cirrus formed and measured at high latitudes (H-H, blue) and cirrus formed and measured at mid-latitudes (M-M). The model output has a time resolution of one hour over the period June-July 2021 to adjust to the backward trajectories time step.

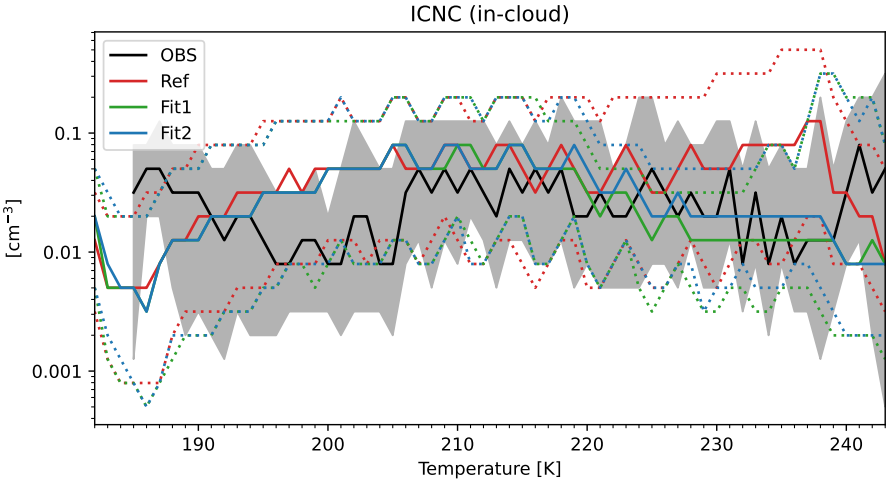

Figure S5. Comparison of simulated in-cloud ice crystal number concentrations from the cases Ref, Fit1, and Fit2 with an observational climatology derived from various flight campaigns (Krämer et al., 2016, 2020), considering the simulated period from 2014-2016. Solid lines show median values, shadings and dotted lines show the 25^{th} to 75^{th} percentile range.